

NHTSA - 98-3588-59

**SAE TECHNICAL  
PAPER SERIES**

DEPT. OF TRANSPORTATION  
DOCKETS

**1999-01-0715**

99 OCT -6 PM 4: 01

65396

---

# Development of A Finite Element Human Thorax Model for Impact Injury Studies

Yih-Charng Deng  
GM Engineering Center

Wayne Kong and Henjen Ho  
GM R&D Center

Reprinted From: Occupant Protection  
(SP-1432)

**SAE** The Engineering Society  
For Advancing Mobility  
Land Sea Air and Space,  
INTERNATIONAL

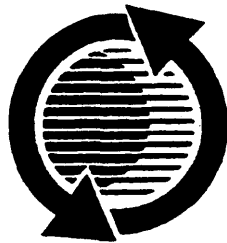
International Congress and Exposition  
Detroit, Michigan  
March 1-4, 1999

The appearance of the ISSN code at the bottom of this page indicates SAE's consent that copies of the paper may be made for personal or internal use of specific clients. This consent is given on the condition however, that the copier pay a \$7.00 per article copy fee through the Copyright Clearance Center, Inc. Operations Center, 222 Rosewood Drive, Danvers, MA 01923 for copying beyond that permitted by Sections 107 or 108 of the U.S. Copyright Law. This consent does not extend to other kinds of copying such as copying for general distribution, for advertising or promotional purposes, for creating new collective works, or for resale.

SAE routinely stocks printed papers for a period of three years following date of publication. Direct your orders to SAE Customer Sales and Satisfaction Department.

Quantity reprint rates can be obtained from the Customer Sales and Satisfaction Department.

To request permission to reprint a technical paper or permission to use copyrighted SAE publications in other works, contact the SAE Publications Group.



**GLOBAL MOBILITY DATABASE**

*All SAE papers, standards, and selected books are abstracted and indexed in the SAE Global Mobility Database.*

No part of this publication may be reproduced in any form, in an electronic retrieval system or otherwise, without the prior **written** permission of the publisher.

**ISSN 0148-7191**

**Copyright ©1999 Society of Automotive Engineers, Inc.**

Positions and opinions advanced in this paper are those of the author(s) and not necessarily those of SAE. The author is solely responsible for the content of the paper. A process is available by which discussions will be printed with the paper if it is published in SAE Transactions. For permission to publish this paper in full or in part, contact the SAE Publications Group.

Persons wishing to submit papers to be considered for presentation or publication through SAE should send the manuscript or a 300 word abstract of a proposed manuscript to: Secretary, Engineering Meetings Board, SAE.

**Printed in USA**

90-1203B/PG

# Development of A Finite Element Human Thorax Model for Impact Injury Studies

**Yih-Chang Deng**

GM Engineering Center

**Wayne Kong and Henjen Ho**

GM R&D Center

Copyright © 1999 Society of Automotive Engineers, Inc.

## ABSTRACT

A finite element human thorax model was developed for predicting thoracic injury and studying the injury mechanisms under impact. Digital surface images of a human skeleton and internal organs were used to construct the three-dimensional finite element representation of the rib cage, the heart, the lungs, and the major blood vessels. The mechanical properties of the biological tissues in this model were based on test data found in the literature. The constitutive equations proposed in the literature for describing the mechanical behavior of the heart and the lungs were implemented in the code for modeling these organs. The model was validated against cadaver responses for both frontal and lateral impact. Good correlation between the model and the cadaver responses were achieved for the force and deflection time-histories.

## INTRODUCTION

Thoracic injury is one of the leading causes of fatalities from automotive crashes. Rib fracture is the most frequent type of thoracic injury, followed by the trauma of the pulmonary/lung, heart and liver[1]. To study injury mechanisms and design countermeasures to improve occupant protection in a crash, various experimental and analytical techniques have been used in the past. Analytical investigation of thoracic injury has been pursued using various modeling approaches. In the early seventies, Lobdell[2] developed a one-dimensional lumped parameter representation of the human thorax. More sophisticated three-dimensional beam-type finite element thorax models were developed by Roberts and Chen[3], and Closkey et al.[4]. The rapid advancement of computer CPU power and the ability to process large

quantities of data led to the development of even more detailed finite element models for the thorax, such as those in Plank et al.[5] and Wang[6]. In Plank et al.[5] the rib cage model was based on the geometric data in Roberts and Chen[3] with rectangular cross section ribs. Each cross sectional area contains four elements and the same cross sectional area was used for all the ribs in the model. The internal organs were represented by a continuum filling the entire thoracic cavity. The viscoelastic parameters of the continuum were adjusted to provide the best match to the cadaver impact response corridors. In Wang's model[6] the heart and the lungs were modeled according to the anatomical geometry and nonlinear stress-strain curves were used to describe the mechanical properties. However, the ribs were modeled using only one element in each cross section. Since single point integration was used in the analysis, one element in the cross section would not provide bending stiffness. The bending stiffness of the rib cage was achieved from the two layers of shell elements attached to the external and internal side of the rib cage simulating the intercostal muscles. These previous efforts, although with limitations and approximations, provided valuable lessons in the pursuit of human body modeling.

The objective of this study is to develop a detailed finite element thorax model with accurate representation of both geometric features and material properties. The finite element mesh of the model was constructed from a commercial data package of human thorax geometry (Viewpoint DataLabs, Orem, Utah). New material models were developed in the Dyna3D code for simulating the mechanical behavior of the biological tissues in the thorax region. The thorax model was validated against cadaver responses in frontal and lateral impacts.

---

. Contract Employee

## THE RIB CAGE MODEL

THE RIB - The rib is composed of two types of bony tissue, the trabecular bone in the middle and the cortical bone on the outer surface. The trabecular bone consists of a three-dimensional interconnected network of trabecular rods and plates. The density varies from 0.1 to 1.3  $\text{g/cm}^3$  [7]. The cortical bone consists of compact bony tissue with a density of 1.3 to 1.8  $\text{g/cm}^3$ . Typical stress-strain curves for these bones contain a linear elastic region, a yield point, a plastic region and a failure point. Previous studies[7] have illustrated that both the Young's modulus and the ultimate strength are rate-dependent. In Dyna3D, material type 19 (strain rate-dependent-plasticity) is suitable for modeling the bone. Failure mechanisms were also included in this model by specifying a failure stress. When the failure stress was reached in an element, this element was deleted in the model. Table 1 depicts the material constants for the cortical and trabecular bones derived from data in Ref. 7. The rate-dependency of the Young's modulus and the ultimate stress was characterized by a straight line in a logarithmic scale according to data in Ref. 7.

Table 1. Material constants for the bone at  $\dot{\epsilon} = 1 \text{ s}^{-1}$ .

	Cortical Bone	Trabecular Bone	Coarse Mesh
Density, $\text{g/cm}^3$	1.8	1.1	1.53
Young's Modulus, GPa	24	0.24	26
Yield Stress, MPa	200	2.0	110
Modulus in the Plastic Region, GPa	2.2	0.022	2
Ultimate Stress, MPa	220	2.2	125

To reflect the structural composition of the rib, it is necessary to use a fine mesh, as shown in Fig. 1, in which each transverse section contains 28 elements with the outer layer of elements simulating the cortical bone and the inner core elements simulating the trabecular bone. However, such a modeling approach for the entire rib cage would be CPU prohibitive even using the most powerful computer available today. To alleviate the CPU burden, a coarser mesh for the rib was developed, as shown in Fig. 1, in which only 8 elements were used in the transverse direction. Clearly, by using such a mesh, it is no longer possible to model the trabecular bone and the cortical bone separately, and material properties for the rib would be a combination of the trabecular bone

and the cortical bone to achieve an equivalent mechanical behavior. To ensure that the coarse mesh model would respond in a similar fashion as the fine mesh model, both models were subjected to a dynamic loading test in which the spinal end of the rib was constrained and the sternal end was pulled toward the spinal end as shown in Fig. 1. A linear displacement-time history was prescribed to the sternal end causing it to move about 144 mm in 30 ms. The material constants used in the fine mesh model are based on values listed in Table 1.

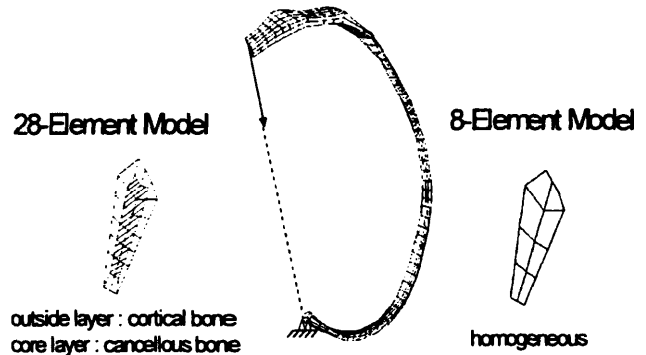
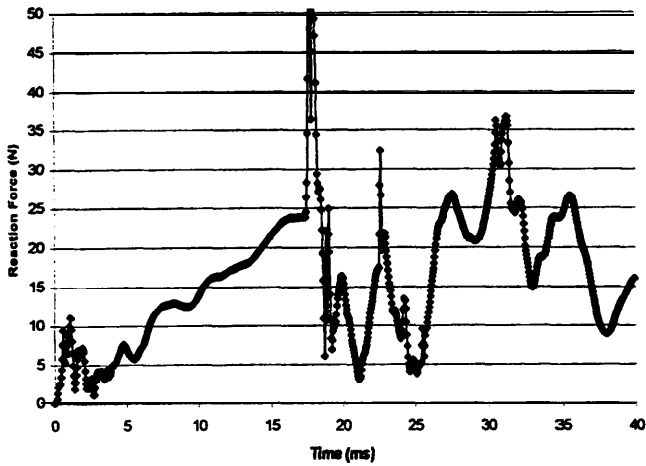
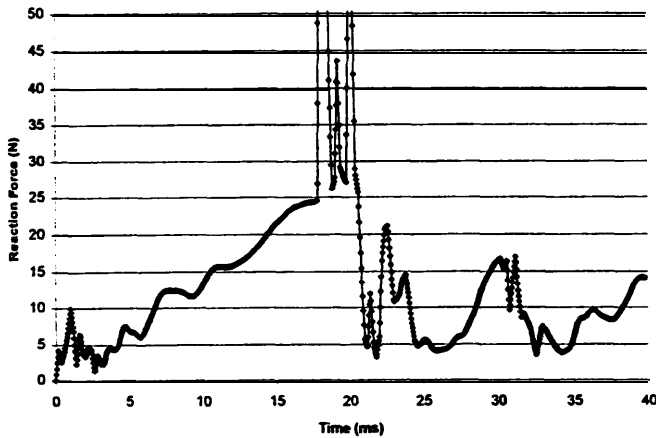


Fig. 1. The single-rib model and the cross-sections for the fine and coarse meshes.

The material constants for the coarse model were first calculated from those of the cortical bone and the trabecular bone based on their proportion in the transverse section. These values were further adjusted to achieve the best correlation with the fine mesh model in this dynamic loading condition. Based on this process, the material constants identified for the coarse mesh model are also listed in Table 1. Figure 2 depicts the time-histories of the reaction force measured at the fixed spinal end of the two rib models. It can be observed that from 0 to 16 ms the rib deformed elastically with an almost linear response. First yield occurred at approximately 16 ms, and first material failure, with the removal of the element, occurred at about 18 ms. Some high frequency oscillations can be observed at the onset of element deletion, suggesting some numerical instability. These oscillations subsided at about 22 ms and the force started to decrease as the sternal end continued to move and more elements were deleted due to material failure. With the selection of suitable material constants for the 8-element model, the similarity between the two models can be readily observed. In the literature, experiments on isolated ribs were conducted by Schultz et al.[8] to characterize their bending stiffness in the rib plane. With 7.35 N load, it was found that the upper ribs deflected about 3 cm while the lower ribs deflected about 6 cm. The rib deflection observed in our models exhibited comparable characteristics as that of Schultz et al..



(a)



(b)

Fig. 2. The force-time curves for a single rib with (a) fine, and (b) coarse meshes.

It is interesting to note that the optimized Young's modulus for the coarse mesh model does not have a value between those of the cortical bone and the trabecular bone. This is due to the fact that a **single-point** integration scheme was used in our model. For the coarse mesh model, the integration points are closer to the center of the cross section than those of the cortical bone in the fine mesh model. **This** led to a reduction of bending stiffness in the coarse mesh model and a higher Young's modulus was needed to compensate for that effect. Single-point integration also imposed a limitation on the failure mechanism in the model. As the sternal end continued to move, more element failures, and hence deletion, was observed in the model. However, when there were only one or two elements remaining in a cross section, it became impossible for the rib to provide a bending stiffness and a complete break of the rib due to bending did not occur. Nonetheless, this numerical limitation does not prevent the model from simulating the impact response of the human thorax and predicting potential rib fractures.

**THE SPINE** - Since the main application of this model is for thoracic injury studies involving rib fracture **and** internal organ injury, the thoracic spine was not modeled with great detail. The thoracic vertebrae were modeled as rigid bodies with cylindrical shapes. The flexibility of the intervertebral disks was modeled by rotational joints with rotational stiffness and damping based on the test data reported by **Panjabi[9]**.

Each rib is connected to the corresponding thoracic vertebra via a rotational joint. Moment-rotation functions were used to simulate the rotational characteristics along the three axes. These functions were derived from Ref. 10 as listed in Table 2. In addition, a simple representation of the cervical spine and the lumbar spine was included. A lumped mass of 4.1 kg was attached to the superior end of the **cervical** spine to simulate the head, and a lumped mass of 40.1 kg was attached to the inferior end of the lumbar spine to simulate the lower torso and the legs. These masses were based on values reported in Ref. 11 for a mid-size male.

Table 2. Rotational stiffness of the spino-costal joints.

Rotational Stiffness ( $\times 10^3$ N-mm/rad)		
X (Ant-Post.)	Y (Left-Right)	Z (Sup.-Inf.)
53	39	72

**THE STERNUM AND CARTILAGE** - The sternum was modeled using the cortical bone properties. The cartilage connecting the sternum and the ribs was modeled as an elastic material with a density of 5.0 **g/cm<sup>3</sup>**, a Young's modulus of 1.2 Gpa, and a Poisson's ratio of 0.2. These material properties were based on data in the **literature[12-13]** for the **articular** cartilage, augmented to account for material transition of **bone-cartilage-bone**. The connection between the cartilage and the sternum was via rotational joints. The characteristics of these joints were based on test data in **Refs. 4 and 10** as listed in Table 3.

Table 3. Rotational stiffness of the **sterno-costal** joints.

Rotational Stiffness ( $\times 10^3$ N-mm/rad)		
X (Ant-Post.)	Y (Left-Right)	Z (Sup.-Inf.)
25	100	25

**THE SOFT TISSUES** - The ribs are connected by the internal and external intercostal muscles. These muscles were modeled by membrane elements to provide force during tension and buckling when in compression. They were modeled using the fabric material model (type 34) in the **Dyna3D** code with a density of 1 **g/cm<sup>3</sup>**, a Young's modulus of 2.5 Mpa, and a Poisson's ratio of 0.4. The value of Young's modulus is based on test data reported by Myers et al.[14] of mammalian muscles *in situ*.

Membrane elements with the same material properties as the intercostal muscles were also used to simulate the diaphragm below the rib cage. The perimeter of the diaphragm was connected to the lower edge of the rib cage. Figure 3 depicts the rib cage model.

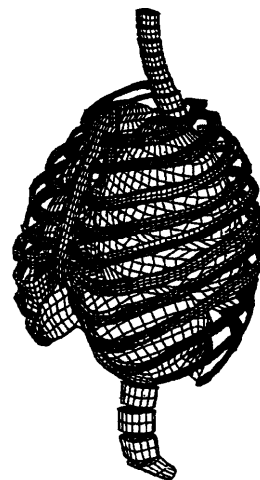


Fig. 3. The rib cage model.

### THE INTERNAL ORGANS

The inside of the rib cage, the heart, the lungs, and the major blood vessels were modeled as described in the following.

**THE HEART** - The heart model was constructed based on the geometric data from Viewpoint **DataLabs**. The heart muscle was modeled with 8-node brick elements as shown in Fig. 4. The four chambers in the heart were also modeled albeit the valve mechanisms were not considered. The blood inside the heart chambers was modeled by an elastic fluid material model shown in Table 4.

Table 4. Material constants of the blood.

Density, <b>g/cm<sup>3</sup></b>	1.0'
Young's Modulus, <b>MPa</b>	1.32
Poisson's Ratio	0.4999
Bulk Modulus, <b>MPa</b>	2200

The material properties of the heart muscle have been investigated extensively in the past and a number of constitutive models have been proposed in the literature. **McCulloch et al.[15]** used a strain energy function,  $W$ , of the following form to simulate the passive behavior of the heart muscle,

$$W = \frac{C}{2}(e^{\rho} - 1) - \frac{p}{2}(I_3 - 1) \quad (1)$$

$$Q = b_1 E_{11}^2 + b_2 (E_{22}^2 + E_{33}^2 + E_{23}^2 + E_{32}^2) + b_3 (E_{12}^2 + E_{21}^2 + E_{13}^2 + E_{31}^2)$$

in which  $E_{ij}$  are Lagrangian strain components,  $p$  is the hydrostatic pressure variable,  $I_3$  is the third principal strain invariant, and  $C$ ,  $b_1$ ,  $b_2$ ,  $b_3$  are constants. This constitutive model was implemented in the **Dyna3D** code for the current study and numerical values of material

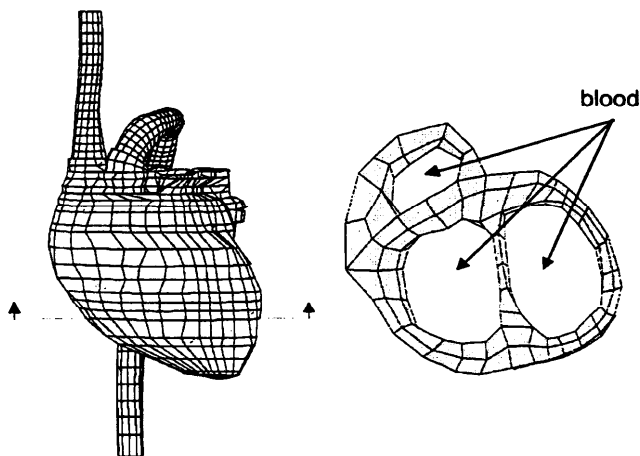


Fig. 4. The heart model.

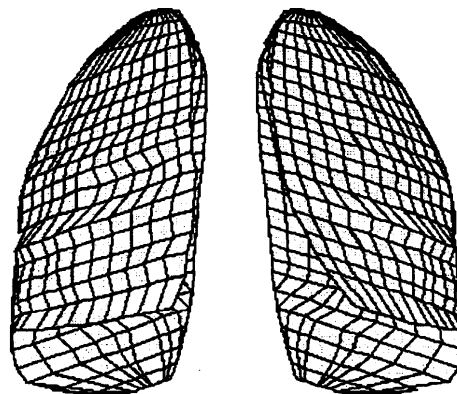


Fig. 5. The lung model.

constants reported by Guccione and McCulloch[16], as shown in Table 5, were used in the model.

Table 5. Material constants of the heart muscle.

C (kPa)	$b_1$	$b_2$	$b_3$
0.88	18.5	3.58	1.63

**THE LUNG** - The lung model was also constructed based on the geometric data from the Viewpoint DataLabs. The lung was modeled with **8-node** brick elements as shown in Fig. 5. The mechanical behavior of the lung parenchyma has also been investigated extensively in the past and constitutive models have been proposed in the literature. For this study, we adopted the approaches developed by Fung et al.[17] and Vawter[18] in which the elastic properties of the lung tissue were modeled by a strain energy function as shown in the first term of Eq. (2). In addition, due to the surfactant and air interaction it has been demonstrated by Vawter[18] that the surface energy also plays a significant role in the lung tissue behavior. Thus, the total strain energy of the lung tissue includes a surface energy part as described by the second term in Eq. (2), i.e.,

$$W = \frac{C}{2\Delta} \exp(\alpha I_1^2 + \beta I_2) + \frac{12C_1}{\Delta(1+C_2)} [A^{(1+C_2)} - 1] \quad (2)$$

$$A^2 = \frac{4}{3}(I_1 + I_2) - 1$$

where C,  $C_1$ ,  $C_2$ ,  $\alpha$ ,  $\beta$  are material constants,  $A$  is the typical alveolar diameter when unstressed, and  $I_1$  and  $I_2$  are the strain invariants. The above constitutive model was implemented in the **Dyna3D** code for this investigation. Material constants listed in Ref. 18 were used in this study as shown in Table 6.

Table 6. Material constants for the lung tissue.

C/A (kPa)	$\alpha$	$\beta$	$C_1/\Delta$ (Pa)	$C_2$
2.45	0.183	-0.291	19.3	2.71

**THE BLOOD VESSELS** - The aorta and the superior vena cava were modeled by shell elements with elastic fluid elements inside to simulate the blood. The blood vessels were modeled by an elastic material with a Young's modulus of 5 MPa and a Poisson's ratio of 0.4. These values were derived from data compiled in Abe et al.[19].

## MODEL VALIDATION

The thorax model was validated by comparing its impact response to test results found in the literature for the frontal impact[20-22] and a series of side impact tests recently conducted at the Wayne State University[23].

**FRONTAL IMPACT** - In the early seventies a series of cadaver tests was conducted to study thoracic injury due to a frontal blow in the sternum area[20,21]. A 15.24-cm (6-inch) diameter pendulum with 23.4 kg mass was used in the test to strike the cadaver with initial velocities of 4.5 m/s and 6.7 m/s. The forces were measured by a load cell mounted on the pendulum and the chest deflection of the cadaver specimen was determined from high speed films. Using these data, force-deflection corridors were developed for each impact speed. These corridors provided the basic characteristics of the human thorax structure for frontal impact. In this study we subjected the model to these impact conditions and compared the model responses to the cadaver test results.

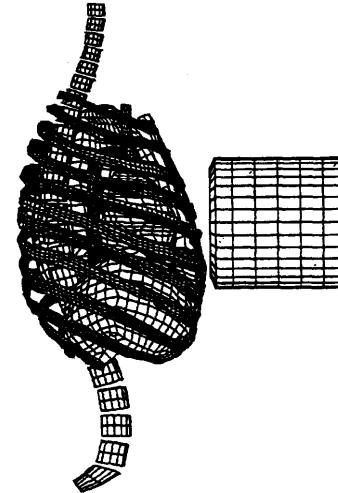
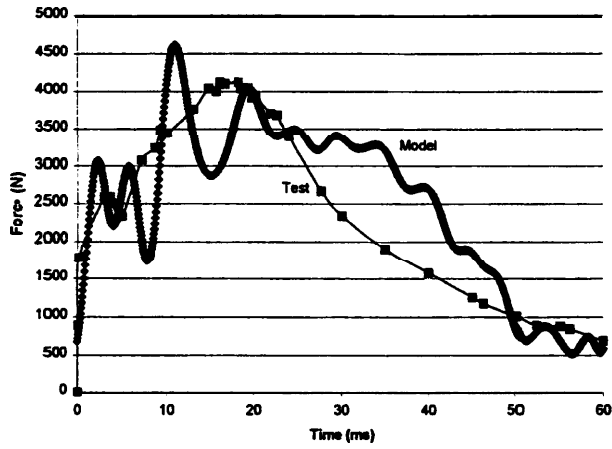
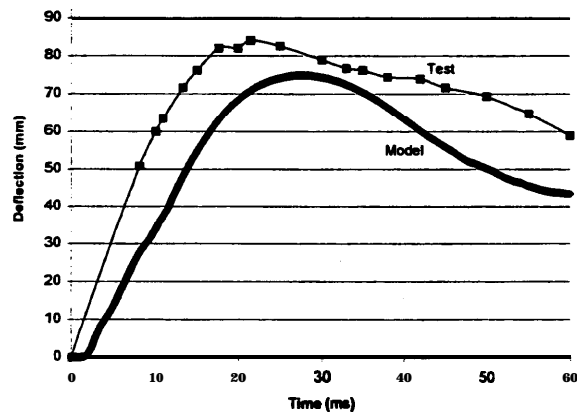


Fig. 6. The frontal impact to the thorax.

As shown in Fig. 6 a rigid cylinder of 15.24-cm (6-inch) diameter and 23.4 kg mass was positioned at the sternum impact location with an initial velocity 6.7 m/s. Following the cadaver test conditions, the model was free to move after impact without any constraint. While the test subjects in Refs. 20 and 21 did exhibit rib fracture, preliminary simulation runs revealed that using the element deletion algorithm to simulate rib fracture led to a drastic weakening of the rib cage structure and excessive rib deformation. Thus, the failure mechanisms in the model were temporarily removed. Before a more rigorous algorithm was developed in the **Dyna3D** for simulating the rib fracture, maximum stresses in the element can be used as indicators of rib fracture. Furthermore, a close examination of the model response revealed excessive rotation at the spino-costal



(a)

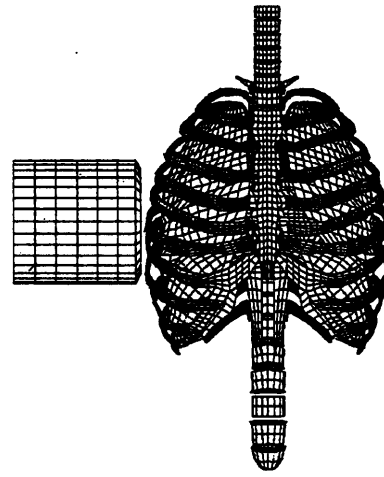


(b)

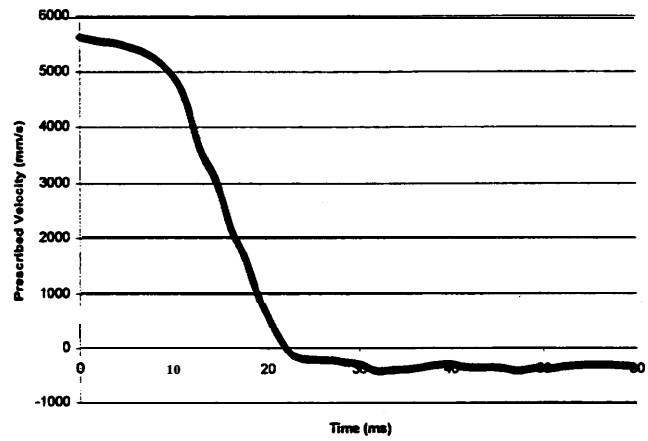
Fig. 7 The model-to-test comparison for frontal impact, (a) force-time history, (b) deflection-time history.

joints. Thus, the rotational stiffness values listed in Table 2 were increased by twofold. This increase can be considered to account for the viscous effect. Figure 7 shows the comparison between the model responses and the cadaver force and deflection responses for the 6.7 m/s impact speed. It can be observed that the model response is close to the cadaver test results.

**SIDE IMPACT** - In addition to the frontal impact validation, attempts were also made to validate the model for side impact. In an on-going research program at Wayne State University sponsored by General Motors, a linear **impactor** was developed which imposes a limited stroke to the side of the cadaver test specimens. The intention of such a device was to mimic the fundamental aspect of a car-to-car impact and study the injury **mechanisms**[24]. To simulate such an impact, the thorax model was struck laterally as shown in Fig. 8a. The center of the **impactor** was aimed at the 6th rib and a velocity-time history shown in Fig. 8b was



(a)



(b)

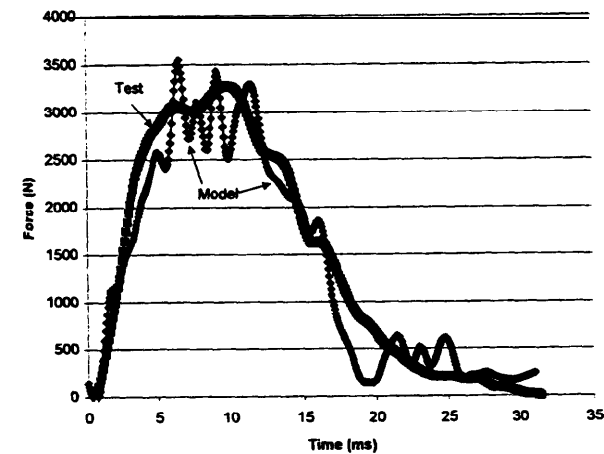
Fig. 8. (a)The side impact to the thorax, (b) **impactor** velocity profile.

prescribed to the **impactor** according to the data recorded in the impact test. Figure 9 illustrates a comparison between the model and the cadaver test for the force and deflection responses. The deflection measurement was calculated from the relative displacement between the right 6th rib and the left 6th rib. It can be observed that the correlation between the model and the test response is satisfactory.

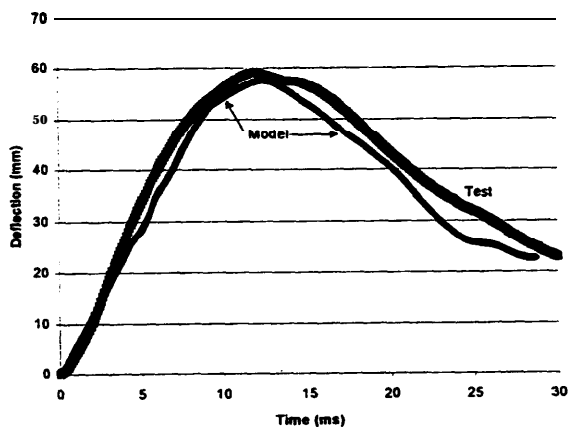
## CONCLUSION

A detailed finite element model of the human thorax was developed for impact injury studies. The model has realistic geometric and material representation of the rib cage, heart and lungs. A modeling procedure was developed to identify suitable material constants for the ribs to account for its composition of cortical bone and trabecular bone. Constitutive equations proposed in the literature for describing the mechanical behavior of the heart muscle and the lung parachema were implemented in the **Dyna3D** program for this study. The

model was validated against cadaver thorax test results for both the frontal and lateral impact. Good correlation was achieved in both conditions for the force and the deflection responses. Further development is currently underway to include the surface muscles, other internal organs and more advanced numerical features for simulating the rib fracture and internal organ injury. Additional analyses will also be carried out for other impact conditions.



(a)



(b)

Fig. 9. The model-to-test comparison for side impact, (a) force-time history, (b) deflection-time history.

## ACKNOWLEDGMENTS

This research is financed by GM pursuant to an agreement between GM and the US Department of Transportation. We'd like to thank Dr. Rolf Eppinger of the NHTSA and Mr. Gordon Plank of **Volpe** for their cooperation and for providing the thorax model in Ref.

[5]. We'd also like to thank LSTC for implementing the new material models used in this study.

## REFERENCES

1. Cavanaugh, J. M., "The Biomechanics of Thoracic Trauma", in *Accidental Injury - Biomechanics and Prevention*, edited by A. M. Nahum and J. W. Melvin, Springer-Verlag, 1993.
2. **Lobdell** T. E., **Kroell**, C. K., Schneider D. C., **Hering**, W. E., and Nahum, A. M., "Impact Response of the Human Thorax", In King, W. F. and **Mertz**, H. J. eds. *Human Impact Response Measurement and Simulation*, Plenum Press, New York, 1973.
3. Roberts, S. B. and Chen, P. H., "Elastostatic Analysis of the Human Thoracic Skeleton", *Journal of Biomechanics* Vol. 3, 1970.
4. Closkey, R. R., Schultz, A. B., and Luchies, C. W., "A Model for Studies of the Deformable Rib Cage", *Journal of Biomechanics*, Vol. 25, 1992.
5. Plank, G. R., Kleinberger, M. Eppinger, R. H., "Finite Element Modeling and Analysis of Thorax/Restraint System Interaction", The 14th International Technical Conference on the Enhanced Safety of Vehicles, Munich, Germany, May 23-26, 1994.
6. Wang, H.-C., "The Development of a Finite Element Human Thoracic Model", **PhD** Dissertation, Wayne State University, 1995.
7. Hayes, W. C., "Biomechanics of Cortical and Trabecular Bone: Implications For Assessment of Fracture Risk", in *Basic Orthopaedic Biomechanics*, Mow, V. C. and Hayes, W. C., eds., Raven Press, New York, 1991.
8. Schultz, A. B., Benson, D. R. and Hirsch, C., "Force-Deformation Properties of Human Ribs", *J. Biomechanics*, Vol. 7, 1974.
9. Panjabi, M., Brand, R. and White, A., "Three Dimensional Flexibility and Stiffness Properties of the Human Thoracic Spine", *J. Biomechanics*, Vol. 9, 1976.
10. Schultz, A. B., Benson, D. R. and Hirsch, C., "Force-Deformation Properties of Human **Costo-Sternal** and **Costo-Vertebral** Articulations", *J. Biomechanics*, Vol. 7, 1974.
11. Schneider, L. W., **Robbins**, D. H., Pflug, M. A. and Snyder, R. G., "Anthropometry of Motor Vehicle Occupants", Volume 1 and 2, The University of Michigan Transportation Research Institute Report **UMTRI-83-53-1** and **UMTRI-83-53-2**, 1983.
12. **Viano**, D. C., "Biomechanics of Bone and Tissue: A Review of Material Properties and Failure Characteristics", SAE Paper 861923, 1986.
13. Mow, V. C., Zhu, W. and **Ratcliffe**, A., "Structure and Function of **Articular** Cartilage and Meniscus", in *Basic Orthopaedic Biomechanics*, Mow, V. C. and Hayes, W. C., eds., Raven Press, New York, 1991.
14. Myers, B. S., Van Ee, C. A., Camacho, D. L. A., Woolley, C. T. and Best, T. M., "On the Structural

- and Material Properties of Mammalian Skeletal Muscle and Its Relevance to Human Cervical Impact Dynamics”, The 39th Stapp Car Crash Conference Proceedings, SAE Paper 952723, 1995.
15. **McCulloch**, A. D. and Omens, J. H., “Non-homogeneous Analysis of Three-dimensional Transmural Finite Deformation in Canine Ventricular Myocardium”, *Journal of Biomechanics*, Vol. 24, 1991.
  16. Guccione, J. M. and **McCulloch**, A. D., “Finite Element Modeling of Ventricular Mechanics”, in *Theory of Heart*, Glass et al. ed., 1991.
  17. Fung, Y.-C., Tong, P., and Patitucci, P., “Stress and Strain in the Lung”, *ASCE Journal of the Engineering Mechanics Division*, 1978.
  18. Vawter, D. L., “A Finite Element Model for Macroscopic Deformation of the Lung”, *Journal of Biomechanical Engineering*, Vol. 102, 1980.
  19. Abe, H., Hayashi, K. and Sato, **M.** (Eds.), *Data Book on Mechanical Properties of Living Cells, Tissues, and Organs*, Springer-Verlag, 1996.
  20. Kroell, C. K., Schneider, D. C. and Nahum, A. M., “Impact Tolerance and Response of the Human Thorax”, in *Biomechanics of Impact Injury and Injury Tolerances of the Thorax-Shoulder Complex*, Backaitis, S. H. ed., SAT Publication PT-45, SAE Paper No. 710851.
  21. Kroell, C. K., Schneider, D. C. and Nahum, A. M., “Impact Tolerance and Response of the Human Thorax II”, in *Biomechanics of Impact Injury and Injury Tolerances of the Thorax-Shoulder Complex*, Backaitis, S. H. ed., SAE Publication PT-45, SAE Paper No. 741187.
  22. **Neathery, R.**, “Analysis of Chest Impact Response Data and Scaled performance Recommendations”, SAE Paper 741188.
  23. “Development of A Human Thorax Model: Human Cadaver Thorax Impact Response”, Wayne State University Annual Report, GM/DOT Settlement Research Docket GMRSRCH. 1998.
  24. Deng, Y.-C., “The Importance of the Test Method in Determining the Effects of Door Padding in Side Impact”, *The 33rd Stapp Car Crash Conference Proceedings*, 1989.